Singularity clustering in the Duffing oscillator

1988 J. Phys. A: Math. Gen. 21 33

(http://iopscience.iop.org/0305-4470/21/1/014)

J. Phys. A: Math. Gen. **21** (1988) 33-54. Printed in the UK

Singularity clustering in the Duffing oscillator

J D Fournier†‡, G Levine§ and M Tabor‖

† Department of Astronomy, Columbia University, New York, NY 10027, USA
§ Department of Physics, Columbia University, New York, NY 10027, USA
‖ Department of Applied Physics, Columbia University, New York, NY 10027, USA

Received 6 October 1986

Abstract. An asymptotic and numerical study is made of the singularity structure, in the complex t-plane, of the Duffing oscillator. The presence of logarithmic terms in the local psi-series expansion, of the form $t^4 \ln t$, leads to a multisheeted singularity structure of great complexity. This structure is built recursively from an elemental pattern which takes the form of four-armed 'stars' of singularities. This construction is deduced analytically from the properties of the mapping $z = t^4 \ln t$ and is confirmed quite accurately numerically. A systematic resummation of the psi series, in terms of Lamé functions, is developed. This series exhibits the same analytic structure at all orders and provides a 'semi-local' *analytical* representation of the solution which is apparently valid even in the chaotic regime.

1. Introduction

The study of the analytic structure of dynamical systems—in particular the singularities exhibited by the solution in the complex time domain—can provide a variety of insights into the properties of the system. Use of what is now termed the 'Painlevé property', namely the property that the only movable singularities exhibited by the solution are ordinary poles, can sometimes provide a direct means of identifying integrable cases of a given system. (A semi-historical review may be found in [1].) However, the study of analytic structure need not be restricted to the search for integrable cases only and the singularity structure of non-integrable systems appears to have a rich content.

In a detailed study of the Lorenz equations, Tabor and Weiss [2] (hereafter referred to as I) found that in the non-integrable regimes the solution could be formally represented near singularities in terms of psi series involving logarithmic terms. By identifying a certain subset of coefficients in these expansions they were able to obtain, through a variety of transformations, an asymptotic picture of the solution in the neighbourhood of a given singularity. In a subsequent numerical study of the Henon-Heiles system Chang *et al* [3] found that in certain system parameter regimes, for which the singularities have complex exponents, the singularities clustered in remarkable self-similar spirals. A detailed theoretical analysis of this phenomenon by Chang *et al* [4] (hereafter referred to as II) was able to provide an accurate description of this geometry. Spirals of singularities were subsequently observed and similarly analysed in a study of the stationary solutions of Kuramoto's equation by Thual and

‡ On leave from CNRS, France. Present and permanent address: CION BP139, 06003 Nice Cedex, France.

0305-4470/88/010033+22$02.50

Frisch [5] and in a certain Hamiltonian system by Yoshida [6]. Despite the apparent self-similarity of the structures observed in II it has been pointed out by Bessis and Chafee [7] that care should be taken in concluding that they correspond to a (possibly fractal) natural boundary since the singularities are distributed over an immensely complicated multi-sheeted Riemann surface.

The question of the precise relationship between actual real time behaviour and complicated singularity structures has also been addressed. A study of a forced non-linear Langevin equation by Morf and Frisch [8] analysed the influence of the singularities nearest the real axis in terms of 'intermittent' excitations of the real solution. Bountis and Segur [9] and Bountis *et al* [10] have suggested that the appearance of (widespread) chaos may be related to the influence of logarithmic branch points and the latter have emphasised the importance of singularity 'condensation' in this process. A similar point of view has been adopted by Dombre *et al* [11] who suggest, on the basis of their analysis of the so-called ABC flows, that recursive singularity clustering is a hallmark of non-integrability. We also remark that a 'condensation' or 'confluence' of simple poles in the complex domain occurs in a variety of physical contexts, such as statistical mechanics [12], fluid mechanics [13], combustion [14], etc. Furthermore Ruelle [15] has recently suggested the value of studying the analytic structure of Fourier transforms—rather than of the signal itself—in which case results by Ruelle and Pollicott exclude any clustering in a meromorphic strip; even for chaotic systems.

In this paper our aim is to make a detailed study of the types of singularity clustering that can occur for logarithmic singularities—similar in spirit to the study of clustering given for complex exponent singularities in II. We choose as our model the Duffing equation

$$\ddot{x} + \lambda \dot{x} + \tfrac{1}{2}x^3 = \varepsilon F(t) \tag{1.1}$$

where λ is a damping coefficient and ε the coupling to the external field $F(t)$—which is taken to be an entire function. This system has proved to be a useful model for a variety of physical processes such as beam buckling [16] and non-linear circuits [17] as well as a popular model for studies of chaotic dynamics [18]. Furthermore it is probably the simplest possible case suitable for our purposes for which detailed analytical (and numerical) studies are possible. This is desirable since logarithmic singularities are present in such important systems as the Lorenz equations, for which the analysis in I is very similar but could not be pushed as far as in the present work. Indeed, here we are able to demonstrate (in §§ 3 and 4) a star-like, recursive singularity structure different from the spiralling structure found in II. This is based on a detailed asymptotic study of the associated psi series. In § 5 we show that this asymptotics is itself only the first term in an expansion made up of Jacobi and Lamé functions. This expansion provides a systematic way of partially resumming the psi series and the singularity structure appears to be the same at any order of this expansion. We feel that these results place our numerical results on firmer ground—even if the exact convergence properties of all these expansions are still unknown.

2. The psi-series expansion

For convenience we write out the four cases of the Duffing equation that are embraced

by our analysis. They are

$$\ddot{x}+\tfrac{1}{2}x^3=0 \tag{2.1}$$

$$\ddot{x}+\lambda\dot{x}+\tfrac{1}{2}x^3=0 \tag{2.2}$$

$$\ddot{x}+\tfrac{1}{2}x^3=\varepsilon F(t) \tag{2.3}$$

$$\ddot{x}+\lambda\dot{x}+\tfrac{1}{2}x^3=\varepsilon F(t). \tag{2.4}$$

Obviously (2.1), (2.2) and (2.3) are just subcases of (2.4) but for reference purposes it is useful to list them separately. The basic properties of these systems may be summarised as follows.

(2.1). This is a conservative Hamiltonian system which can be integrated exactly in terms of the Jacobi elliptic functions. The motion is completely regular.

(2.2). This non-Hamiltonian system has a stable spiral point at the origin to which all initial conditions tend in the limit $t\to\infty$. Although the motion is completely regular we are not aware of an explicit quadrature to provide an 'exact' solution to the equations of motion.

(2.3). This is a non-conservative Hamiltonian system. For sufficiently strong coupling, ε, to an external periodic field, e.g. $F(t)=\cos(\Omega t)$, the solutions can exhibit chaotic behaviour.

(2.4). The presence of both dissipation and driving can lead to the appearance of a stable limit cycle. As ε is increased this cycle can undergo 'universal' period doubling bifurcations leading to a 'strange attractor'. Detailed dynamical studies have been made by Ueda [18].

We remark that the traditional Duffing equation usually contains a linear term in the restoring force—however this neither affects the dynamics nor our analysis. We also note that the λ dependence of (2.4) can be scaled away. Using the scalings $x(t)=\lambda y(\lambda t)$, $F(t/\lambda)=G(t)$ and $\delta=\varepsilon/\lambda^3$ we obtain

$$\ddot{y}+\dot{y}+\tfrac{1}{2}y^3=\delta G(t).$$

For computational purposes it is convenient to work with the unscaled equations.

It is an easy matter to show that about an arbitrary movable singularity t_0, in the complex t-plane, the solution to (2.1) may be locally represented as a simple Laurent series of the form

$$x(t)=\sum_{j=0}^{\infty} a_j(t-t_0)^{j-1}. \tag{2.5}$$

Direct substitution of (2.5) into the equations of motion leads to the recursion relations for the a_j

$$a_j(j+1)(j-4)=-\tfrac{1}{2}\sum_k\sum_l a_{j-k-l}a_k a_l \qquad 0<k+l\leqslant j,\ 0\leqslant k,\ l<j \tag{2.6}$$

where $a_0=2\mathrm{i}$, $a_1=a_2=a_3=0$, $a_4=$ arbitrary coefficient, etc. The arbitrary pole position t_0 and coefficient a_4 constitute the two pieces of arbitrary data consistent with a local representation of the general solution to the second-order equation (2.1). As mentioned above, this equation can be solved exactly in terms of the Jacobi elliptic functions and the movable singularities in the complex t-plane form a regular lattice of first-order poles.

The introduction of either dissipation (2.2) or driving (2.3) (or, of course, both (2.4)) leads to the breakdown of the Laurent series (2.5) since it becomes no longer

possible to introduce an arbitrary coefficient at $j=4$. It is again a standard matter (see, for example, Bender and Orszag [19]) to rectify this problem by adding logarithmic terms to the expansion thereby obtaining the psi series

$$x(t)=\sum_{j=0}^{\infty}\sum_{k=0}^{\infty}a_{jk}(t-t_0)^{j-1}((t-t_0)^4\ln(t-t_0))^k. \tag{2.7}$$

Computation of the recursion relations for the a_{jk} is tedious but straightforward and one obtains, for the general case (2.4),

$$\begin{aligned}a_{jk}((j-1)(j-2)+4k(2j+4k-3))&+a_{j-4,k+1}(k+1)(2j+8k-3)\\&+a_{j-8,k+2}(k+1)(k+2)+\lambda a_{j-1,k}(j+4k-2)+\lambda a_{j-5,k+1}(k+1)\\&=-\tfrac{1}{2}\sum_{\substack{p,q,\\r,s}}a_{j-r,k-s}a_{r-p,s-q}a_{pq}+\varepsilon F_{j-3}\delta_{k0}\end{aligned} \tag{2.8}$$

where the summation is for $0\leq p\leq r\leq j$ and $0\leq q\leq s\leq k$ and where

$$F_j=\frac{1}{j!}\frac{\partial^j F}{\partial t^j}\bigg|_{t=t_0}.$$

The values of the first few coefficients in (2.8) are easily found to be

$$a_{00}=2\mathrm{i}\qquad a_{10}=-\mathrm{i}\lambda/3\qquad a_{20}=-\mathrm{i}\lambda^2/18\qquad a_{30}=-\mathrm{i}\lambda^3/27-\varepsilon F_0/4.$$

There are resonances for a_{40} and a_{01}; a_{40} is the compatibility condition of the resonance imposing the choice of a_{01}, namely

$$a_{01}=4\mathrm{i}\lambda^4/135+\tfrac{1}{5}\varepsilon(\lambda F_0+F_1).$$

The value of the coefficient a_{01} plays a particularly significant role in all of the subsequent analysis. Again t_0 and a_{40} constitute the two pieces of arbitrary data entering into the (formally) self-consistent expansion (2.7).

Following the procedure described in I we now look for a closed set of recursion relations amongst the a_{jk}. These are the set a_{0k}, $k=0,1,2,\ldots$, which satisfy

$$4k(k-1)a_{0k}+ka_{0k}+\tfrac{1}{2}a_{0k}=-\tfrac{1}{8}\sum_s\sum_q a_{0,k-s}a_{0,s-q}a_{0q} \tag{2.9}$$

where the summation is for $0\leq q\leq s\leq k$. Introducing the generating function

$$\Theta(z)=\sum_{k=0}^{\infty}a_{0k}z^k \tag{2.10}$$

where z is some (as yet unspecified) independent variable, the following differential equation for $\Theta(z)$ is obtained:

$$16z^2\Theta''(z)+4z\Theta'(z)+2\Theta(z)+\tfrac{1}{2}\Theta^3(z)=0 \tag{2.11}$$

where the prime denotes differentiation with respect to z. (This is, to within a trivial scaling, identical to equation (A5) obtained in I.)

The differential equation (2.11) may be obtained via a different, more direct, route using the procedure described in II. In the limit $t\to t_0$ we concentrate on the terms in the psi series (2.7) involving powers of $t^4\ln t$ and therefore make the substitution

$$x(t)=\frac{1}{t-t_0}\Theta_0(z) \tag{2.12}$$

where

$$z = (t - t_0)^4 \ln(t - t_0) \tag{2.13}$$

into equation (2.4) (or for that matter equations (2.3) or (2.2)). In the limit $t \to t_0$ it is easy to show formally that $\Theta_0(z)$ again satisfies equation (2.11), provided that there is an ordering in which $|t - t_0| \ll |z|$. Due to the infinite multivaluedness of the logarithm this is indeed perfectly possible for large (absolute) values of the argument of $(t - t_0)$. We remark that for a psi series involving complex powers, i.e. $z = (t - t_0)^\alpha$, where α is the relevant complex exponent, one can provide similar arguments (see II) to justify the dominance of these terms in the limit $t \to t_0$. In both situations this asymptotic approach and the closed recursion relations approach yield the same equation. Moreover, according to our numerical explorations, the validity of the result deduced in this way is not limited to high-index sheets of the Riemann t-surface. A partial explanation of this success is given in § 5, where we study a systematic resummation of the psi series in terms of a certain set of functions of z—of which Θ_0 is the leading term (hence the subscript zero). In this section we just concentrate on the properties of Θ_0. Finally, we also comment that this approach can be thought of as a type of 'renormalisation' in that the differential equation (2.11) can be regarded as the original equation of motion 'rescaled' in the neighbourhood of a given singularity. However, it is interesting to note that now (2.11) possesses the 'Painlevé property' since it is easily demonstrated that about an arbitrary movable singularity (say at $z = z_0$) $\Theta_0(z)$ has the Laurent series expansion

$$\Theta_0(z) = \pm 8 \mathrm{i} z_0 \sum_j A_j (z - z_0)^{j-1} \tag{2.14}$$

where (see also I)

$$A_0 = 1 \qquad A_1 = \frac{5}{8z_0} \qquad A_2 = -\frac{5}{64 z_0^2} \qquad A_3 = \frac{5}{128 z_0^3} \qquad A_4 = \text{arbitrary}.$$

Remarkably equation (2.11) may be integrated exactly in terms of elliptic functions by making the substitution

$$\Theta_0(z) = z^{1/4} f(z^{1/4}) \tag{2.15}$$

which leads to the equation

$$f''(y) + \tfrac{1}{2} f^3(y) = 0 \tag{2.16}$$

where the prime denotes differentiation with respect to the variable $y = z^{1/4} = t(\ln t)^{1/4}$. In keeping with the idea of 'renormalisation' we again stress that through the two-step transformation ((2.12) and (2.15)) the general Duffing equation (2.4) has been locally mapped onto the integrable case (2.1) (identical to (2.16)). We now proceed to the complete solution of (2.16). The first integral of (2.16) is just

$$(f')^2 + \tfrac{1}{4} f^4 = I_1 \tag{2.17}$$

where one may determine that $I_1 = -20\mathrm{i}a_{01}$. By means of the simple scaling $f(y) = 2(I_1/4)^{1/4} g((I_1/4)^{1/4} y)$ (2.17) is reduced to the standard form for integration in terms of elliptic functions yielding

$$g(\bar{y}) = \pm \mathrm{i}\sqrt{2}\, \mathrm{ds}(\sqrt{2}(\bar{y} - \bar{y}_0)) \tag{2.18}$$

where $\bar{y}_0$ is some initial phase and the elliptic function parameter $m = \frac{1}{2}$ (lemniscate case). The function $\mathrm{ds}(u)$ has the standard (see the appendix for a summary of pertinent results) rectangular lattice of (first-order) poles with real and imaginary periods $4K(\frac{1}{2})$ and $4\mathrm{i}K'(\frac{1}{2})$ where K and K' are the standard modulus and complementary modulus respectively. For this particular case $K = K'$ and hence the poles lie on a square lattice with spacing $2K$. Back on the y-plane the function $f(y)$ has the same lattice but scaled and rotated about the origin in the y-plane by an amount determined by the (in general) complex-valued first integral I_1. The compatibility of the asymptotic behaviour of Θ_0, f and g for $z \to 0$, $y \to 0$, $\bar{y} \to \bar{y}_0$, imposes the choice $\bar{y}_0 = 0$ and the value $I_1 = -20\mathrm{i}a_{01}$. Thus finally one has

$$f(y) = \mathrm{i}\frac{4\lambda}{3^{3/4}}\left(1 - \frac{27\mathrm{i}\varepsilon}{4\lambda^4}(\lambda F_0 + F_1)\right)^{1/4} \mathrm{ds}\left[\frac{2\lambda}{3^{3/4}}\left(1 - \frac{27\mathrm{i}\varepsilon}{4\lambda^4}(\lambda F_0 + F_1)\right)^{1/4} y\right]. \tag{2.19}$$

The pole positions, labelled by the lattice site integers l, m, are given by

$$y_{lm} = \tau_{lm} \ln^{1/4} \tau_{lm} = \frac{(27)^{1/4}}{\lambda} K(\tfrac{1}{2})\left(1 - \frac{27\mathrm{i}\varepsilon}{4\lambda^4}(\lambda F_0 + F_1)\right)^{-1/4} (l + \mathrm{i}m) \qquad l, m \in Z \tag{2.20}$$

where τ_{lm} are the corresponding positions in the t-plane.

From these results the following picture of singularity clustering emerges. To each singularity t_0 in the complex t-domain one can attach an associated y-plane. The lattice of singularities in the y-plane, as given by (2.20), is then mapped (back) into the t-space according to the multivalued transformation $z = t^4 \ln t$. An immensely complicated, multisheeted structure in the t-space can be envisaged with the degree of clustering (about a given t_0) determined by both the degree of 'scaling' and 'rotating' in the y-plane and the intricacies of the mapping $z \to t$. Furthermore any one of these singularities in the t-space can have its own clustered sub-structure. The recursive nature of this clustering can clearly lead to a singularity structure of pathological complexity. Some preliminary numerical results, which strikingly confirm our predictions, will be described later. Despite this complexity there is a rather remarkable feature of the above analysis. Combining equations (2.12), (2.15) and (2.19) leads to an explicit local expression for $x(t)$ which accurately predicts the location and nature of neighbouring singularities. Coupled with the higher-order terms (described in § 5) this therefore provides, in effect, an integration of motion traditionally regarded as 'non-integrable' and, for some parameter values, even known to exhibit chaos.

There are a variety of subcases of the general result (2.19) and (2.20) that we mention explicitly.

(i) $\lambda \neq 0$, $\varepsilon = 0$, i.e. system (2.2). Here the first integral of (2.17) is $I_1 = 16\lambda^4/27$ and one obtains

$$f(y) = \mathrm{i}\frac{4\lambda}{3^{3/4}} \mathrm{ds}\left(\frac{2\lambda}{3^{3/4}} y\right) \tag{2.21a}$$

$$y_{lm} = \tau_{lm} \ln^{1/4} \tau_{lm} = \frac{3^{3/4}}{\lambda} K(\tfrac{1}{2})(l + \mathrm{i}m). \tag{2.21b}$$

In this case the fundamental lattice is shrunk (or dilated) but not rotated. However, the numerical results seem to show that there is *no* singularity clustering in the complex t-domain according to this scheme. Since clustering is observed for all the other cases this suggests here that either the local transformation (2.12) is in some sense global

or that the radius of convergence of the asymptotic analysis is always less than the distance of the nearest poles to the origin of the y-plane.

(ii) $\lambda = 0$, $\varepsilon \neq 0$, i.e. system (2.3). Here the first integral of (2.17) is $I_1 = -4i\varepsilon F_1$ and one obtains

$$f(y) = 2i\sqrt{2}\, e^{-i\pi/8}(\varepsilon F_1)^{1/4}\, ds[\sqrt{2}\, e^{-i\pi/8}(\varepsilon F_1)^{1/4} y] \tag{2.22a}$$

$$y_{lm} = \tau_{lm} \ln^{1/4} \tau_{lm} = \frac{\sqrt{2}\, e^{+i\pi/8}}{(\varepsilon F_1)^{1/4}} K(\tfrac{1}{2})(l + im). \tag{2.22b}$$

Now the fundamental lattice is both shrunk (or dilated) and rotated. Clearly the exact value of F_1 plays an important role. For those cases where it is zero the expansion about t_0 reverts to a pure Laurent series. This can either occur for (*a*) $F(t) =$ constant—in which case (2.2) is integrable in terms of elliptic functions—or (*b*) a freak value of t_0 for non-trivial $F(t)$.

(iii) $\lambda \neq 0$, $\varepsilon \neq 0$, i.e. the general system (2.4). There are a couple of interesting subcases here.

(*a*) $-\lambda F_0 = F_1$: the lattice 'distortion' is reduced to a simple scaling, i.e.

$$y_{lm} = \tau_{lm} \ln^{1/4} \tau_{lm} = (27^{1/4}/\lambda) K(\tfrac{1}{2})(l + im). \tag{2.23}$$

Such a situation could arise for a driving force of the form $F(t) = A\, e^{-\lambda t}$.

(*b*) $4\lambda^4/27i = \varepsilon(\lambda F_0 + F_1)$: this corresponds to a_{01} in (2.7) vanishing, i.e. the singularity is locally meromorphic. In this case Θ_0, in (2.12), reverts to the role of the leading-order coefficient $\Theta_0 = a_{00} = 2i$.

3. The mapping function $z = t^4 \ln t$

A crucial part of our analysis is to determine the way in which the lattice of poles in the $y = z^{1/4}$ plane maps back into the t-plane. For convenience we set the pole position $t_0 = 0$ in (2.13) and work with

$$z = t^4 \ln t. \tag{3.1}$$

The trick is to use polar coordinates in both the z- and t-planes. Setting

$$z = \rho\, e^{i\varphi} \tag{3.2}$$

and

$$t = r\, e^{i\vartheta} \tag{3.3}$$

we have from (3.1) that

$$\operatorname{Re} z = r^4[\cos(4\vartheta) \ln r - (\vartheta + 2\pi n) \sin(4\vartheta)] \tag{3.4a}$$

$$\operatorname{Im} z = r^4[\sin(4\vartheta) \ln r + (\vartheta + 2\pi n) \cos(4\vartheta)] \tag{3.4b}$$

where n is the Riemann sheet index in the t-plane. From this pair of equations one may easily determine that

$$\tan\varphi = \tan(4\vartheta)\left(\frac{\ln r + (\vartheta + 2\pi n)\cot(4\vartheta)}{\ln r - (\vartheta + 2\pi n)\tan(4\vartheta)}\right)$$

and hence

$$r = e^{-(\vartheta + 2\pi n)\cot(4\vartheta - \varphi)}. \tag{3.5}$$

Using this result in (say) equation (3.4*a*) one may then deduce that

$$\rho = -(\vartheta + 2\pi n)\, e^{-4(\vartheta+2\pi n)\cot(4\vartheta-\varphi)}(\sin(4\vartheta-\varphi))^{-1}. \tag{3.6}$$

The pair of equations (3.5) and (3.6) completely determine the mapping. A given pole in the y-plane is assigned polar coordinates ρ', φ' (where $y = \rho' e^{i\varphi'}$) from which $\rho = (\rho')^4$ and $\varphi = 4\varphi'$ are readily computed. From (3.6) one may then 'read off' (in practice this corresponds to a simple numerical root search) the value of ϑ, for any sheet n, corresponding to the given (ρ, φ) values. From this value of ϑ the associated radial coordinate r is computed from equation (3.5). In figure 1, we plot the function $\rho(\vartheta)$ against ϑ, for the ϑ range $(\varphi/4, 2\pi + \varphi/4)$, for the choice $n = 0$ and with $\varphi \neq 0$. As expected θ is a four-valued function of ρ (the negative branches are ignored since ρ is positive) although it is not quite periodic due to the $\vartheta + 2\pi n$ pre-exponential factor. For a fixed n the effect of changing φ on $\rho(\vartheta)$ is merely to shift the whole function. For a fixed φ the effect of changing n is most significant (although almost imperceptible on a plot such as figure 1) for small n. The following mapping picture emerges: a given pole in the y-plane maps to four points in the t-plane for each sheet. The cumulative effect for large positive n is a four arm 'star-like' structure as shown in figure 2 (for the model choice $\rho = 1$, $\varphi = 0$). As can be seen from this diagram the star is not perfectly symmetrical—the arms have a slight twist and the singularities become more densely 'packed' along each arm as they approach the centre of the star as n increases. The same overall picture would, of course, emerge for large negative n thereby providing a 'mirror image' of the positive n structure.

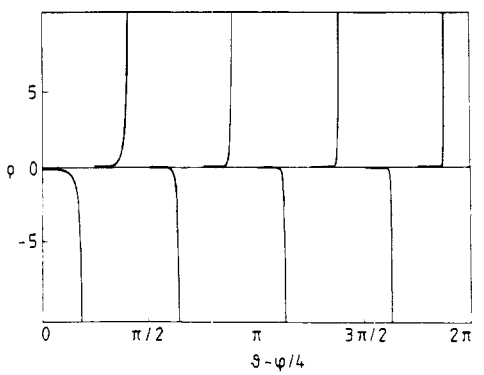

Figure 1. Plot of $\rho(\theta)$ against θ as determined by equation (3.6).

Some analytical estimates of the 'star' geometry can be obtained in the following way. From figure 1 we see, to a first approximation, that $\rho(\theta)$ is either zero or infinity. Thus it is reasonable to study the behaviour of $\rho(\theta)$ at those points for which $\cos(4\theta - \varphi) = 0$, i.e.

$$\theta \simeq \frac{\varphi}{4} + \frac{\pi}{8} + m\frac{\pi}{4} \qquad m = 1, 3, 5, 7 \ldots$$

where the m is chosen to keep the angle in the correct quadrant. Now for this angle we may deduce from (3.6) that

$$r = \frac{|\rho|^{1/4}}{\left|\frac{1}{4}\varphi + \frac{1}{8}\pi + \frac{1}{4}m\pi\right|^{1/4}}.$$

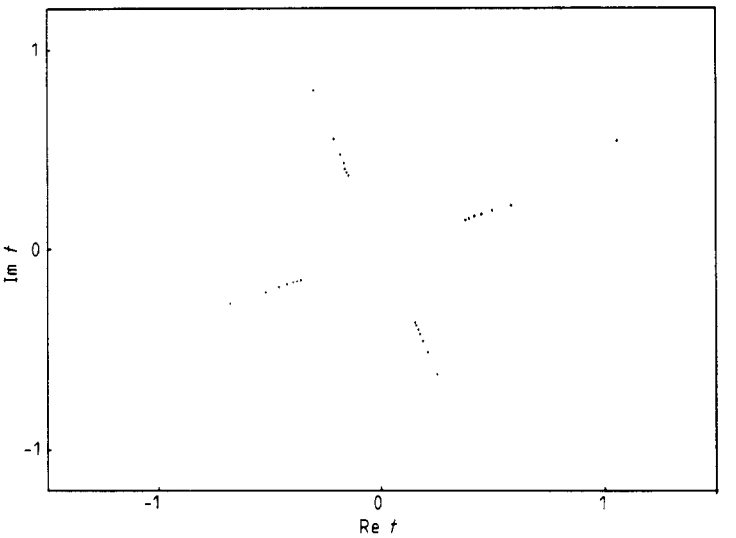

Figure 2. Result of mapping a single pole from the y-plane to the t-plane using equation (3.6) for model choice of $\rho = 1$, $\varphi = 0$.

In order to consider the changes in r along any one arm of the star we must set $m = 8p$ and thereby obtain

$$r_p = r_0\left(\left|1+\frac{16\pi p}{2\varphi+3\pi}\right|\right)^{-1/4}$$

where

$$r_0 = \frac{|\rho|^{1/4}}{|\frac{1}{4}\varphi+\frac{3}{8}\pi|^{1/4}}.$$

Choosing the particular case $\varphi = 0$ enables us to see that $r_p = r_0|1+16p/3|^{-1/4}$—an estimate that is born out well by the numerical results. This result also suggests that

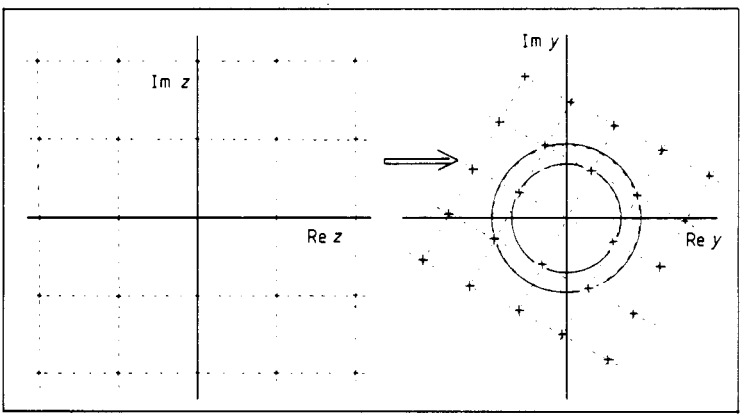

Figure 3. Schematic representation of the way in which the standard lattice of poles can be shrunk and rotated in the y-plane (as determined by equation (2.20)). Note that the poles form families of four that can be inscribed in circles of increasing radius.

in the limit $p \to \infty$, $r_p \to 0$, the arms will, albeit very slowly, gradually reach the central singularity t_0. However, it should be recalled that each member of a given arm is on a different sheet or that this accumulation corresponds to (infinite) multivaluation near t_0.

It seems reasonable to assume that the singularities nearest the y-plane origin (equivalent to the point t_0 in the t-plane) will play the dominant role in determining the t-plane structure. Since the lattice of poles in the y-plane (even after scaling and rotation) is square, the poles form sets of four which may be inscribed in circles of given radius ρ'. Furthermore the members of each set become equivalent under the transformation $z = y^4$ and thus one only requires the radius (i.e. ρ') of each circle of poles and their orientation (i.e. φ'). This idea is sketched diagrammatically in figure 3. In practice (see § 4) we find that mapping just the first two circles of poles is in general sufficient to explain the observed singularity structure.

4. Numerical results

For our numerical studies of the singularity structure of the Duffing equation in the complex t-plane we have used a version of the ATOMCC integrator, developed by Chang and Corliss [20], implemented in double precision, on an IBM PC-XT. With this program it is possible to integrate an ordinary differential equation on any piecewise linear path in the complex t-plane. At each step the program reports the solution and the position and order of the nearest singularity. By suitable choice of integration paths one can build up a picture of the complex t-plane on any scale desired.

In figure 4 we show a portion of the complex t-plane for the completely integrable system (2.1). The program reproduces, to a high degree of accuracy, the expected square lattice of first-order poles. The periodicity of the real time oscillations (not shown here) is, in keeping with standard results, twice that of the pole spacing.

In figure 5 we display a typical t-domain picture for the damped oscillator (2.2). As the damping λ is added the singularities are 'swept' away from the real axis in the manner shown. To leading order the singularities are first-order poles but, as expected, are demonstrably multivalued when repeated circuits are made about them. As mentioned in § 2 no singularity clustering was detected in our numerical studies.

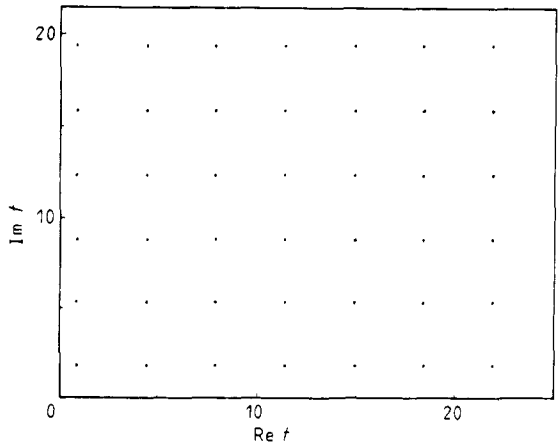

Figure 4. Square lattice of poles found in typical solution of (2.1) using ATOMCC.

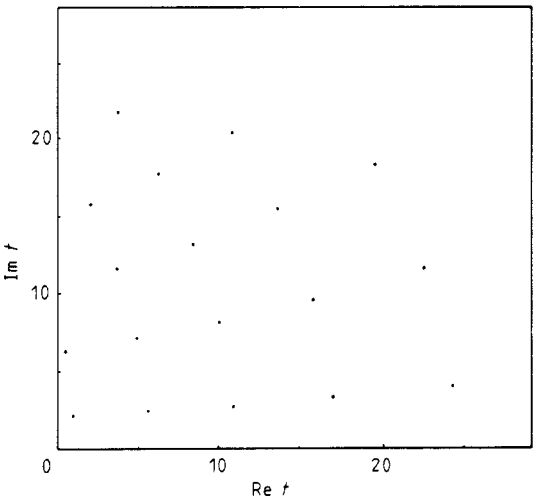

Figure 5. Singularity distribution in the complex t-domain of a solution to the damped oscillator (2.2) with $\lambda = 0.1$.

Almost all of the following numerical results have been obtained with the undamped driven system (2.3) since this is the case for which further analytical results, as described in the next section, have been obtained. Numerical results for the damped driven equation (2.4) show the same basic features as those described below and for completeness we just show one such result later on. A typical 'global' complex t-domain structure for equation (2.3) is shown in figure 6. As the driving term is added the regular lattice gradually distorts into the structure shown. It is important to note that the singularities shown forming the main 'tunnel' structures are all on the lowest Riemann sheet—this is ensured by starting all integration paths on the real axis and checking that no path goes around any of the singularities as they are detected. The 'chimney-like' structure seems to be characteristic of non-integrable systems. It was observed for the Henon-Heiles system [3] and more recently for the Duffing equation [10]. Although our primary concern here is with local structure we comment in passing

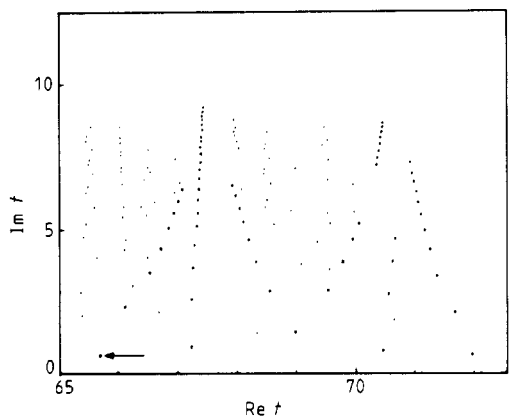

Figure 6. Typical singularity distribution in complex t-domain for a solution of the undamped Duffing oscillator (2.3) with $\varepsilon = 5.0$. Accentuated poles (heavy dots) indicate commonly observed 'tunnel' structures.

that these chimneys appear, on the basis of simple analytical arguments, to close at an exponential rate.

We now look, in figure 7, at the detailed, local structure in the neighbourhood of the singularity marked with the arrow in figure 6. The picture is built up by making careful repeated circuits of the 'central' singularity. The star-like structure observed can be explained in terms of the mapping described in the previous section. The five 'arms' of singularities correspond to a set of three (at 10, 1 and 4 o'clock) and a set of two (at 11 and 2 o'clock). The former set are three out of the four arms obtained by mapping the circle of poles nearest the origin of the corresponding z-plane back onto the t-plane. The other two are part of the 'star' obtained from next-nearest singularity set in the z-plane. If formulae (2.22), with the corresponding parameter values, are used to determine the precise scale and orientation of the y-plane lattice the star-like patterns generated in the t-domain by solving the mapping equations (3.5) and (3.6) are in good agreement with the observed numerical solutions. The fact that some of the 'arms' are missing in figure 7 seems to be some artefact associated with (as yet not understood) difficulties in taking ATOMCC along integration paths across the real axis.

A critical test of our clustering theory is that it should be recursive. This is nicely confirmed in figure 8. Here the detailed structure in the neighbourhood of the arrowed

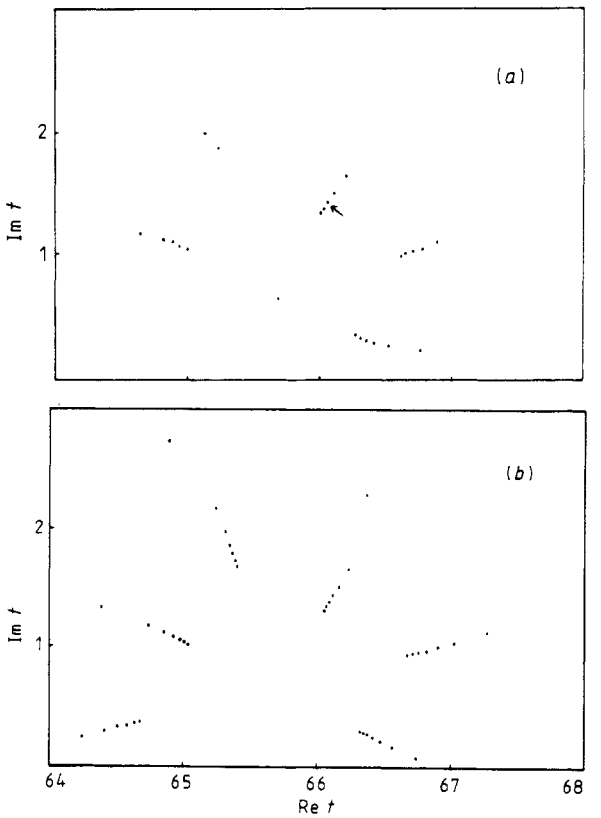

Figure 7. (*a*) Detailed local singularity structure, found using ATOMCC, in neighbourhood of marked singularity in figure 6. (*b*) Local singularity structure determined from the analytical mapping (3.6) with the parameters in (2.20) being chosen to correspond with the actual numerical results of (*a*).

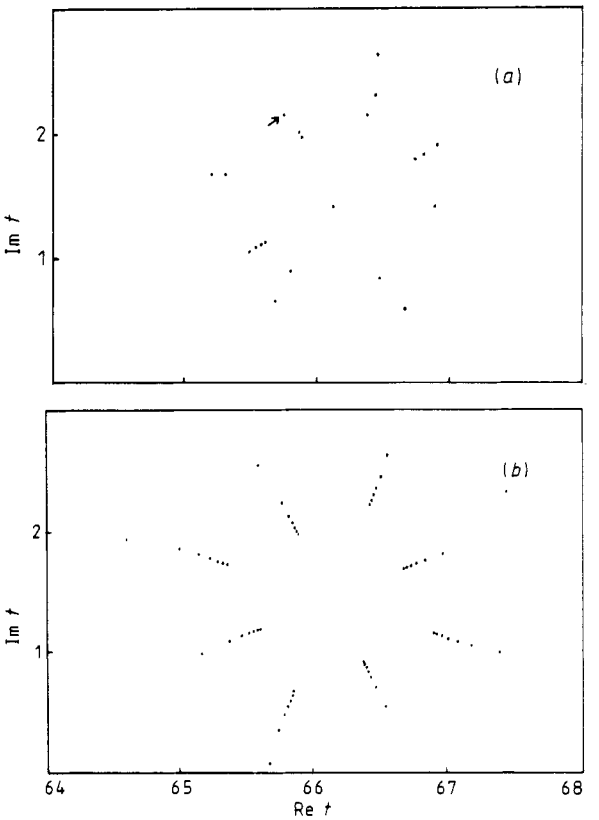

Figure 8. (*a*) Detailed local singularity structure, found using ATOMCC, in neighbourhood of marked singularity in figure 7(*a*). (*b*) Corresponding structure determined by analytical mapping.

singularity in figure 7 is shown. The scale and orientation of the eight 'arms' of singularities agree well with the results obtained from the mapping theory when the nearest and next-nearest (to the origin of the associated y-plane) singularities are used. Further confirmation of the recursive nature of the clustering is provided by figure 9 which shows the neighbourhood of the arrowed singularity in figure 8. Here only one four-arm 'star' was detected—but again its scale and orientation were found to be in good agreement with the mapping theory. Finally, in figure 10 we show a case of clustering for $\lambda \neq 0$—again good agreement between theory and numerical experiment is obtained.

A rather remarkable feature of the agreement between the numerical results and the clustering theory based on the mapping (3.1) is that it should work over such large portions of the t-domain with apparently little regard to the (presumably small) radius of convergence of the original psi series (2.7). This is a matter that clearly deserves further investigation.

5. An alternative asymptotic expansion

As alluded to in the previous section the substitution (2.12) can be thought of as just

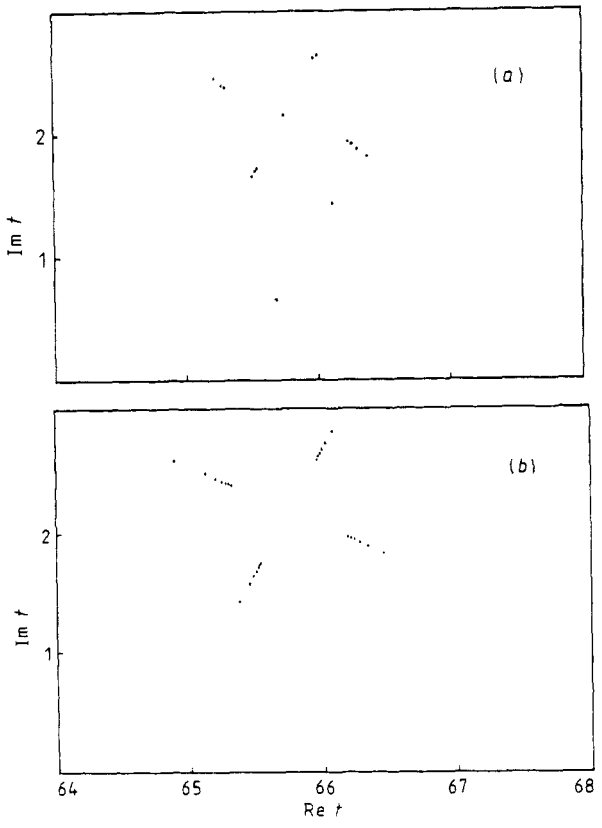

Figure 9. (*a*) Detailed local singularity structure, found using ATOMCC, in the neighbourhood of the marked singularity in figure 8(*a*). (*b*) Corresponding structure determined by analytical mapping.

the first term in a more general expansion of the form

$$x(t)=\sum_{k=0}^{\infty}\Theta_k(z)t^{k-1} \tag{5.1}$$

where $z=t^4\ln t$ and for notational convenience we have set $t_0=0$. Substitution of (5.1) into any of (2.2), (2.3) or (2.4) and taking the limit $t\to 0$ leads to a hierarchy of coupled differential equations for the Θ_k, i.e.

$$k=0 \qquad 16z^2\ddot{\Theta}_0+4z\dot{\Theta}_0+2\Theta_0+\tfrac{1}{2}\Theta_0^3=0 \tag{5.2a}$$

$$k=1 \qquad 16z^2\ddot{\Theta}_1+12z\dot{\Theta}_1+\tfrac{3}{2}\Theta_1\Theta_0^2=\lambda(\Theta_0-4z\dot{\Theta}_0) \tag{5.2b}$$

$$k=2 \qquad 16z^2\ddot{\Theta}_2+20z\dot{\Theta}_2+\tfrac{3}{2}\Theta_2\Theta_0^2=-\lambda 4z\dot{\Theta}_1-\tfrac{3}{2}\Theta_0\Theta_1^2 \tag{5.2c}$$

$$k=3 \qquad 16z^2\ddot{\Theta}_k+4(2k+1)z\dot{\Theta}_k+[(k-1)(k-2)+\tfrac{3}{2}\Theta_0^2]\Theta_k$$
$$=-\lambda[(k-2)\Theta_{k-1}+4z\dot{\Theta}_{k-1}]-\tfrac{1}{2}\sum_m\sum_n\Theta_{k-m}\Theta_{m-n}\Theta_n+\varepsilon F_{k-3} \tag{5.2d}$$

....

All the differential equations for $\Theta_k k\geqslant 1$ are linear inhomogeneous equations. The general homogeneous counterpart is just

$$16z^2\ddot{\Theta}_k+4(2k+1)z\dot{\Theta}_k+[\tfrac{3}{2}\Theta_0^2+(k-1)(k-2)]\Theta_k=0 \qquad k\geqslant 1. \tag{5.3}$$

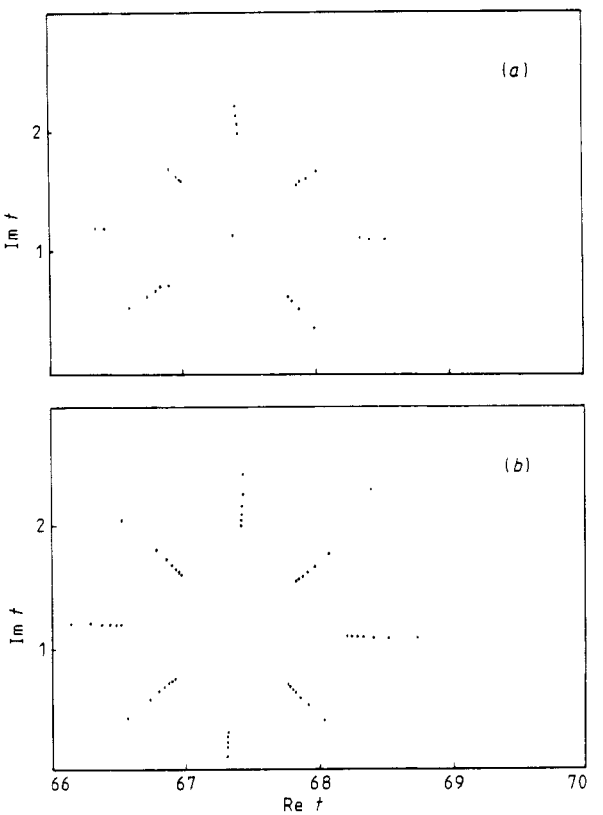

Figure 10. (*a*) Typical local singularity structure, found using ATOMCC for damped, driven oscillator (2.4) with $\lambda = 0.1$, $\varepsilon = 5.0$. (*b*) Corresponding structure determined by analytical mapping.

Remarkably this equation can be solved exactly by making the substitution

$$\Theta_k(z) = (z^{1/4})^{1-k}\psi_k(z^{1/4}) \qquad k \geqslant 0 \tag{5.4}$$

which, with a little manipulation, reduces (5.3) to

$$\ddot{\psi}_k + \tfrac{3}{2}\psi_0^2\psi_k = 0 \tag{5.5}$$

for the functions ψ_k, $k \geqslant 1$. Now from § 2 we have $\psi_0(y) \equiv f(y) = 2\mathrm{i}\sigma C x_0(Cy)$ where C is some scaling factor and x_0 is the Jacobi function ds with $m = \frac{1}{2}$. Thus

$$\ddot{\psi}_k(y) - 6C^2\,\mathrm{ds}^2(Cy)\psi_k(y) = 0 \qquad k \geqslant 1.$$

Equation (5.5) is further simplified by the global rescaling $\psi_k(y) = 2\mathrm{i}\sigma C x_k(Cy)$ and the identity $\mathscr{P}(\xi) = \mathrm{ds}^2(\xi)$, where $\mathscr{P}(\xi)$ is the Weierstrass elliptic function. The function $x_k(\xi)$, solution of the homogeneous counterpart of system (5.2), satisfies

$$\frac{1}{x_k}\ddot{x}_k = a(a+1)\mathscr{P} \qquad a = 2,\ k \geqslant 1 \tag{5.6}$$

a form of the Lamé equation [21] for which a variety of standard results are readily available [21, 22]. For equation (5.6), standard Fuchsian theory [22] tells us that there is one solution of the form

$$x_k^{(1)}(\xi) = (\xi - 2q\omega - 2q'\omega')^{a+1} W(\xi) \qquad q, q' \in Z \tag{5.7}$$

where ω and ω' are the fundamental periods of $\mathcal{P}(\xi)$ and $W(\xi)$ is analytic in the domain of the point $2q\omega + 2q'\omega'$ and not zero at that point. The second solution is given by

$$x_k^{(2)}(\xi) = x_k^{(1)}(\xi) \int \frac{d\xi}{\{x_k^{(1)}(\xi)\}^2}. \tag{5.8}$$

Thus $x_k(\xi)$ can either have third-order zeros, i.e.

$$x_k(\xi) \sim (\xi - \xi_c)^3 \tag{5.9a}$$

or second-order poles, i.e.

$$x_k(\xi) \sim (\xi - \xi_c)^{-2} \tag{5.9b}$$

where ξ_c is one of the lattice sites $2q\omega + 2q'\omega'$ or the origin (i.e. $\xi_c = 0$). At first sight this latter result is rather perturbing since it suggests that the solution, as represented by the series (5.1), could exhibit second-order poles whereas the original differential equation can support only first-order singularities. However, it turns out that the presence of the inhomogeneous terms in the full equations (5.2) cause some remarkable cancellations that nullify this problem. In the case of the non-dissipative driven system, i.e. equation (2.3), we are able to demonstrate this explicitly to sufficiently high order in k to suggest that it is a general result and hence establish the validity of the expansion (5.1).

Applying the various changes of variable and scalings described above to the hierarchy of inhomogeneous equations (5.2) with $\lambda = 0$, we obtain for the functions $x_k(\xi)$,

$$k = 0 \qquad \ddot{x}_0 - 2x_0^3 = 0 \tag{5.10a}$$

$$k = 1 \qquad \ddot{x}_1 - 6x_0^2 x_1 = 0 \tag{5.10b}$$

$$k = 2 \qquad \ddot{x}_2 - 6x_0^2 x_2 = 6x_0 x_1^2 \tag{5.10c}$$

$$k = 3 \qquad \ddot{x}_3 - 6x_0^2 x_3 = -\tfrac{1}{2} i\sigma\varepsilon F^0 / C^3 + 12x_0 x_1 x_2 + 2x_1^3 \tag{5.10d}$$

$$k = 4 \qquad \ddot{x}_4 - 6x_0^2 x_4 = -\frac{1}{2} i\sigma\varepsilon \frac{F^1}{C^4}\xi + \frac{1}{4}\frac{1}{\xi^2} x_0 - \frac{3}{4}\frac{1}{\xi}\dot{x}_0 - \tfrac{1}{2}\ddot{x}_0 + 12x_0 x_1 x_3 + 6x_1^2 x_2 + 6x_0 x_2^2 \tag{5.10e}$$

$$k \geq 5 \qquad \ddot{x}_k - 6x_0^2 x_k = R_k(\xi) \tag{5.10f}$$

where

$$R_k(\xi) = -\frac{i}{2}\sigma\varepsilon \frac{F_{k-3}\xi^{k-3}}{C^k} - \left[\frac{k-5}{4}\right]\frac{1}{\xi^2} x_{k-4} + \left[\frac{2k-11}{4}\right]\frac{1}{\xi}\dot{x}_{k-4} - \tfrac{1}{2}\ddot{x}_{k-4} - \frac{(k-9)(k-5)}{16}\frac{1}{\xi^2} x_{k-8} + \left[\frac{2k-15}{16}\right]\frac{1}{\xi}\dot{x}_{k-8} - \tfrac{1}{16}\ddot{x}_{k-8} + 2 \sum_{\substack{h \\ k>h,l,m\geq 0 \\ h+l+m=k}} \sum_{l} \sum_{m} x_h x_l x_m. \tag{5.10g}$$

In order for the expansion (5.1) to have consistent analytic properties we must seek those Θ_k that are regular at the origin $z = 0$ and whose possible singularities

elsewhere are simple poles. In terms of the x_k this means that at pole positions ξ_c

$$x_k(\xi) \underset{\xi\to\xi_c}{=} O(\xi-\xi_c)^{-1} \tag{5.11a}$$

where $\xi_c \neq 0$ and at $\xi = 0$

$$x_k(\xi) \underset{\xi\to 0}{=} O(\xi^{k-1}). \tag{5.11b}$$

Indeed for the latter case we may write

$$x_k(\xi) \underset{\xi\to 0}{\simeq} \overline{x_k}\xi^{k-1} \tag{5.11c}$$

where

$$\overline{x_k} = -\tfrac{1}{2}\mathrm{i}\sigma C^{-k}\Theta_k(0). \tag{5.11d}$$

The (particular) solution to the general inhomogeneous equation (5.10*f*) takes the standard form

$$x_k(\xi) = -x_{\mathrm{I}}\int^{\xi}\frac{x_{\mathrm{II}}(t)R_k(t)}{\Delta(t)}\,\mathrm{d}t + x_{\mathrm{II}}\int^{\xi}\frac{x_{\mathrm{I}}(t)R_k(t)}{\Delta(t)}\,\mathrm{d}t \tag{5.12}$$

where $x_{\mathrm{I}}(\xi)$ and $x_{\mathrm{II}}(\xi)$ are two, linearly independent, solutions to the associated homogeneous problem and

$$\Delta(\xi) = x_{\mathrm{I}}(\xi)\dot{x}_{\mathrm{II}}(\xi) - x_{\mathrm{II}}(\xi)\dot{x}_{\mathrm{I}}(\xi)$$

is the Wronskian. It is a straightforward matter to show that

$$x_{\mathrm{I}}(\xi) = \mathrm{d}\dot{s}(\xi) \tag{5.13a}$$

is a solution (take the derivative of (5.10*a*), for which ds is a solution, of § 2).

We then write (cf (5.8))

$$x_{\mathrm{II}}(\xi) = H(\xi)x_{\mathrm{I}}(\xi). \tag{5.13b}$$

Up to a multiplicative constant $H(\xi)$ has to satisfy $\dot{H}(\xi) = 1/(\mathrm{d}\dot{s}(\xi))^2$.

In the appendix we show that

$$H(\xi) = (1+\mathrm{i})\frac{\pi}{2K} - 2\xi - \frac{2\,\mathrm{d}s(\xi)}{\mathrm{d}\dot{s}(\xi)} \tag{5.14}$$

is a solution; on dropping the constant terms and multiplicative factors we can redefine

$$x_{\mathrm{I}}(\xi) = \mathrm{d}\dot{s}(\xi) \tag{5.15a}$$

$$x_{\mathrm{II}}(\xi) = \overline{\dot{\xi}\,\mathrm{d}\dot{s}(\xi)} \tag{5.15b}$$

with

$$\Delta(\xi) = -\tfrac{1}{2}. \tag{5.15c}$$

The overbar in (5.15*b*) denotes that all terms under it should be differentiated WRT ξ. (This is not the most elegant notation but makes some of the ensuing expressions more compact.) Using the results (5.15) the solution (5.12) takes the form

$$x_k(\xi) = 2\,\mathrm{d}\dot{s}\int^{\xi} x_{\mathrm{II}}(t)R_k(t)\,\mathrm{d}t - 2\overline{\dot{\xi}\,\mathrm{d}\dot{s}}\int^{\xi} x_{\mathrm{I}}(t)R_k(t)\,\mathrm{d}t. \tag{5.16}$$

Using this result we can now analyse the system of equations (5.10) and determine the conditions under which their solutions behave in the desired fashion, i.e. no singularity at $\xi = 0$ and only *simple* poles elsewhere.

$k = 1$ (5.10*b*). Here $R_1 = 0$ and the only linear combination of x_I and x_{II} which satisfies the required behaviour is the trivial one

$$x_1(\xi) = 0. \tag{5.17}$$

$k = 2$ (5.10*c*). Here $R_2 = 0$ by virtue of (5.17) and again we have the trivial result

$$x_2(\xi) = 0. \tag{5.18}$$

$k = 3$ (5.10*d*). With (5.17) and (5.18) R_3 is a constant, i.e.

$$R_3(\xi) = -\tfrac{1}{2}\mathrm{i}\sigma\varepsilon F_0 / C^3.$$

The general solution is thus

$$x_3(\xi) = -2R_3[\mathrm{d}s^2 - \mu_1\,\mathrm{d}\dot{s} + \mu_2\overline{\xi\,\mathrm{d}\dot{s}}] \tag{5.19}$$

where μ_1 and μ_2 are constants of integration. To ensure regularity at $\xi = 0$ (some useful expansions are listed in the appendix) one must have $\mu_1 = -1$. Thus (5.19) becomes

$$x_3(\xi) = -2R_3(\mathrm{d}s^2 + \mathrm{d}\dot{s}) - 2\mu_2 R_3\overline{\xi\,\mathrm{d}\dot{s}} \tag{5.20}$$

where the first term on the right-hand side is an entire function and the second term can exhibit second-order poles. To remove this feature we must set $\mu_2 = 0$ thereby obtaining

$$x_3(\xi) = \mathrm{i}\sigma\varepsilon\frac{F_0}{C^3}[\mathrm{d}s^2(\xi) + \mathrm{d}\dot{s}(\xi)] \tag{5.21}$$

which is an entire function.

$k = 4$. By virtue of the above results (5.10*e*) now takes the form

$$\ddot{x}_k - 6x_0^2 x_4 = -\tfrac{1}{2}\mathrm{i}\sigma\varepsilon\frac{F_1\xi}{C^4} + \frac{1}{4\xi^2}x_0 - \frac{3}{4\xi}\dot{x}_0 - \tfrac{1}{2}\ddot{x}_0 \tag{5.22}$$

and we look for a solution behaving as

$$x_4 \underset{\xi\to 0}{\simeq} \overline{x_4}\xi^3 + \ldots.$$

The left-hand side of (5.22) for small ξ behaves as

$$6\bar{x}_4\xi - 6\frac{1}{\xi^2}\bar{x}_4\xi^3 + \mathrm{O}(\xi^2) = \mathrm{O}(\xi^2) \tag{5.23}$$

and the right-hand side behaves as (using the Laurent expansion for ds given in the appendix)

$$-\frac{\mathrm{i}}{2}\sigma\varepsilon\frac{F_1}{C^4}\xi + \frac{1}{4}\left[\frac{1}{\xi^3} + \frac{1}{40}\xi\right] - \frac{3}{4}\left[-\frac{1}{\xi^3} + \frac{3}{40}\xi\right] - \frac{1}{2}\left[\frac{2}{\xi^3} + \frac{3}{20}\xi\right] + \mathrm{O}(\xi^2)$$
$$= \left[-\mathrm{i}\sigma\varepsilon\frac{F^1}{C^4} - \frac{1}{4}\right]\frac{1}{2}\xi + \mathrm{O}(\xi^2). \tag{5.24}$$

The compatibility of (5.23) and (5.24) is ensured if and only if

$$C = \sqrt{2}(-\mathrm{i}\sigma\varepsilon F_1)^{1/4}. \tag{5.25}$$

Thus the 'free' constant C has now been fixed in terms of the forcing function. Furthermore use of (5.22) now ensures that near any other singularity ξ_c ($\xi_c \neq 0$) of $x_0(\xi) = \mathrm{d}s(\xi)$, x_4 behaves as

$$x_4(\xi) \simeq \tfrac{1}{4}(\xi - \xi_c)^{-1} \tag{5.26}$$

which is the desired result. (Note that a vanishing F_1 leads to a breakdown of the results.)

$k \geq 5$. The above arguments can be applied to all the ensuing equations, i.e. $k \geq 5$. However an explicit proof that the functions x_k ($k \geq 5$) behave in the desired manner becomes ever more tedious since for each k one needs to know the explicit form of the preceding functions and we did not succeed in finding a recurrence type proof. To summarise we claim the general behaviour is as follows:

$$x_k(\xi) \text{ entire with } x_k(\xi) \underset{\xi \to \xi_c}{=} \mathrm{O}(\xi - \xi_c)^2 \text{ if } k \neq 0 \pmod 4$$

and

$$x_k(\xi) \text{ meromorphic with } x_k(\xi) \underset{\xi \to \xi_c}{=} \mathrm{O}(\xi - \xi_c)^{-1} \text{ if } k = 0 \pmod 4$$

where ξ_c ($\xi_c \neq 0$) is a pole of the Jacobi elliptic function and

$$x_k(\xi) \underset{\xi \to 0}{\simeq} \overline{x_k}\, \xi^{k-1}$$

where $\overline{x_k}$ is defined in (5.11d). Thus collecting all the above results we claim that $x(t)$ can be represented as

$$x(t) = 2\mathrm{i}\sigma C(\ln t)^{1/4}\left(\mathrm{d}s(Ct(\ln t)^{1/4}) + \sum_{k \geq 3} (\ln t)^{-k/4} x_k(Ct(\ln t)^{1/4})\right). \tag{5.27}$$

An instructive way of regarding the expansion (5.1) is to compare it directly with the psi-series expansion (2.7) and recognise that each Θ_j is the generating function for the set of coefficients a_{jk}, i.e.

$$\Theta_j(z) = \sum_{k=0}^{\infty} a_{jk} z^k \tag{5.28}$$

where $z = t^4 \ln t$. For the case $j = 0$ the recursion relations for the a_{0k} are closed whereas for all other cases they are coupled to preceding coefficients. From this point of view we may regard (5.27) as a resummation of the psi series (2.7). Furthermore the properties of the table of coefficients a_{jk} provides additional confirmation of the analysis in this section. Thus, for example, for the case considered here, i.e. the system (2.3), the columns of coefficients a_{1k} and a_{2k}, $k = 0, \ldots, \infty$, are all found from (2.8) to be zero thereby confirming our conclusion that $x_1 = x_2 = 0$.

Acknowledgments

The authors thank D Bessis, T Bountis, Y F Chang, M D Kruskal, A C Newell and I C Percival for useful discussions. This work is supported by the Department of Energy (grant DEFG02-84ER13190). JDF was supported in part by NSF contract PHY 80-2371 and the Office of Naval Research (grant N00014-85-K-0239). MT is an Alfred P Sloan Research Fellow.

Appendix

We first summarise the basic properties of the Jacobi ds function. (Our primary source is Abramowitz and Stegun [23] which we will denote by AS followed by the relevant equation number where appropriate.)

For the Lemniscate case, $m = \frac{1}{2}$, one has (AS 16.9.4)

$$\mathrm{d}s^2 = \frac{\mathrm{d}n^2}{sn^2} = \frac{1 - \frac{1}{2}sn^2}{sn^2} = \frac{1}{sn^2} - \frac{1}{2}$$

and for the associated Weierstrass function $\mathscr{P}$

$$\mathscr{P} = e_3 + \frac{e_1 - e_3}{sn^2[z(e_1 - e_3)^{1/2}]}$$

with (AS 18.14)

$$e_2 = 0 \qquad e_1 + e_3 = 0 \qquad e_1 - e_3 = 1$$

and hence

$$\mathscr{P} = \mathrm{d}s^2$$

with the moduli (AS 18.14)

$$K(\tfrac{1}{2}) = \omega = K'(\tfrac{1}{2}) = 1.854\ldots.$$

For $m = \frac{1}{2}$, the two moduli are equal, the function ds is odd and its poles and zeros are on a double square lattice. The basic spacing is $2K$ and the function periodic with period $4K$, $4\mathrm{i}K'$, $2K + 2\mathrm{i}K'$. Finally it is easy to show (using AS 16.16) that ds satisfies the differential equation

$$\mathrm{d}\ddot{s} = 2\,\mathrm{d}s^3$$

for $m = \frac{1}{2}$.

We now turn to the derivation of equation (5.14). Up to multiplicative constant $H(\xi)$ must satisfy

$$\dot{H}(\xi) = \frac{1}{(\mathrm{d}\dot{s})^2}.$$

For the case $m = \frac{1}{2}$ one has (AS 16.9, 16.16)

$$\frac{1}{(\mathrm{d}\dot{s})^2} = \frac{1}{cs^2 ns^2} = sc^2 sn^2 = (nc^2 - 1)(1 - cn^2) = nc^2 + cn^2 - 2.$$

Using a change of argument (AS 16.8) this can be rewritten as

$$\frac{1}{(\mathrm{d}\dot{s})^2} = 2[\mathrm{d}s^2(\xi - K) - \mathrm{d}s^2(\xi - \mathrm{i}K) - 1]$$

which on using the result $\mathscr{P} = \mathrm{d}s^2$ and the definition $\mathscr{P} = -\dot{\xi}$ finally yields

$$H(\xi) = 2[-\xi(\xi - K) + \xi(\xi - \mathrm{i}K) - \xi]$$

up to an additive constant. From the pseudo-addition law (AS 18.4.3) and the values of the half periods in the lemniscate case (AS 18.14.8-10) this can be written as

$$H(\xi) = 2\left((1 + \mathrm{i})\frac{\pi}{4K} - \xi - \frac{1}{2}\frac{\dot{\mathscr{P}}}{\mathscr{P} - \frac{1}{2}} + \frac{1}{2}\frac{\dot{\mathscr{P}}}{\mathscr{P} + \frac{1}{2}}\right).$$

Again using the particular properties of the $m=\frac{1}{2}$ case for the differential equation satisfied by $\mathscr{P}$, i.e.

$$\dot{\mathscr{P}}^2 = 4\mathscr{P}[\mathscr{P}^2 - \tfrac{1}{4}]$$

and the relation $\mathscr{P} = \mathrm{d}s^2$ enables one to obtain

$$H(\xi) = 2\left((1+\mathrm{i})\frac{\pi}{4K} - \xi - \frac{\mathrm{d}s(\xi)}{\dot{\mathrm{d}}s(\xi)}\right)$$

which is the desired result.

Finally we list the expansions of the Jacobi function $\mathrm{d}s$ with $m=\frac{1}{2}$ in the neighbourhood of any pole z_c. (Here z means $z - z_c$.)

$$\mathrm{d}s(z) = \frac{1}{z} + \frac{1}{40}z^3 + \frac{1}{9600}z^7 + \frac{1}{2\times 10^6}z^{11} + \mathrm{O}(z^{15})$$

$$\dot{\mathrm{d}}s(z) = -\frac{1}{z^2} + \frac{3}{40}z^2 + \frac{7}{9600}z^6 + \frac{11}{2\times 10^6}z^{10} + \mathrm{O}(z^{14})$$

$$\ddot{\mathrm{d}}s(z) = \frac{2}{z^3} + \frac{3}{20}z + \mathrm{O}(z^5)$$

$$[\mathrm{d}s(z)]^2 = \frac{1}{z^2} + \frac{1}{20}z^2 + \mathrm{O}(z^6).$$

In the neighbourhood of any pole $z_c \neq 0$

$$z\,\mathrm{d}s(z) = \frac{z_c}{z - z_c} + 1 + \frac{z_c}{40}(z - z_c)^3 + \frac{1}{40}(z - z_c)^4 + \mathrm{O}[(z - z_c)^7]$$

$$\overline{z\,\mathrm{d}s(z)}^{\cdot} = -\frac{z_c}{(z - z_c)^2} + \frac{3z_c}{40}(z - z_c)^2 + \frac{1}{10}(z - z_c)^3 + \mathrm{O}[(z - z_c)^6].$$

In the neighbourhood of zero

$$z\,\mathrm{d}s(z) = 1 + \frac{1}{40}z^4 + \frac{1}{9600}z^4 + \frac{11}{2\times 10^6}z^{12} + \mathrm{O}(z^{16})$$

$$\overline{z\,\mathrm{d}s(z)}^{\cdot} = \frac{1}{10}z^3 + \frac{1}{1200}z^7 + \frac{6}{10^6}z^{11} + \mathrm{O}(z^{15}).$$

References

[1] Tabor M 1984 *Nature* **310** 277-82
[2] Tabor M and Weiss J 1981 *Phys. Rev.* A **24** 2157-67
[3] Chang Y F, Tabor M and Weiss J 1982 *J. Math. Phys.* **23** 531-8
[4] Chang Y F, Greene J M, Tabor M and Weiss J 1983 *Physica* **8D** 183-207
[5] Thual O and Frisch U 1984 *Workshop on Combustion Flames and Fires, Les Houches, France*
[6] Yoshida H 1984 *Chaos and Statistical Methods* ed Y Kuramoto (Berlin: Springer) p 42
[7] Bessis D and Chafee N 1986 *Chaotic Dynamics and Fractals* ed M F Barnsley and S G Demko (New York: Academic) p 69
[8] Morf R H and Frisch U 1981 *Phys. Rev.* A **23** 2673
[9] Bountis T and Segur H 1982 *AIP Conf. Proc.* vol 88, ed M Tabor and Y Treve (New York: AIP)
[10] Bountis T, Papageorgion V and Bier M 1987 *Physica* **24D** 292-304

[11] Dombre T, Frisch U, Greene J M, Henon M, Mehr M and Soward A M 1986 *J. Fluid Mech.* **167** 353-91
[12] Lee T D and Yang C N 1952 *Phys. Rev.* **87** 410-9
[13] Bessis D and Fournier J D 1984 *J. Physique Lett.* **45** L833-41
[14] Thual O, Frisch U and Henon M 1985 *J. Physique* **46** 1485-94
[15] Ruelle D 1986 *Phys. Rev. Lett.* **56** 405-7
[16] Holmes P 1979 *Phil. Trans. R. Soc.* A **292** 417-48
[17] Ueda Y 1978 *Trans. IEE Japan* **98A** 167-73
[18] Ueda Y 1980 *Ann. NY Acad. Sci.* **357** 422-34
[19] Bender C M and Orszag S A 1978 *Advanced Mathematical Methods for Scientists and Engineers* (New York: McGraw-Hill)
[20] Chang Y F and Corliss G 1980 *J. Inst. Math. Appl.* **25** 349
[21] Forsyth A R 1959 *Theory of Differential Equations* vol 4 (New York: Dover)
[22] Ince E L 1956 *Ordinary Differential Equations* (New York: Dover)
[23] Abramowitz M and Stegun I A 1965 *Handbook of Mathematical Functions* (New York: Dover)